

Time scales of particle clustering in turbulent flows

J. Bec,¹ L. Biferale,² M. Cencini,³ A. Lanotte,⁴ S. Musacchio,⁵ and F. Toschi⁶

¹*CNRS UMR6202, Observatoire de la Côte d'Azur, BP4229, 06304 Nice Cedex 4, France.*

²*Dept. of Physics and INFN, University of Rome "Tor Vergata",
Via della Ricerca Scientifica 1, 00133 Roma, Italy.*

³*INFN-CNR, SMC Dept. of Physics, University of Rome "La Sapienza", Piazzale A. Moro 2,
00185 Roma, Italy, and CNR-ISC, Via dei Taurini 19, 00185 Roma, Italy.*

⁴*CNR-ISAC and INFN, Sezione di Lecce, Str. Prov. Lecce-Monteroni, 73100 Lecce, Italy.*

⁵*INLN, 1361 Route des Lucioles, 06560 Valbonne, France.*

⁶*CNR-IAC, Viale del Policlinico 137, 00161 Roma, Italy, and INFN,
Sezione di Ferrara, Via G. Saragat 1, 44100 Ferrara, Italy.*

(Dated: July 19,2006)

Spatial distributions of heavy particles suspended in an incompressible turbulent flow are investigated by means of high resolution direct numerical simulations. In the dissipative range, it is shown that particles form fractal clusters with properties independent of the Reynolds number. Clustering is there optimal when particle response time is of the order of the Kolmogorov eddy turnover time. In the inertial range, the particle distribution is not scale-invariant anymore. It is however shown that deviations from uniformity depends only on a rescaled contraction rate, and not on the local Stokes number given by dimensional analysis. Particle distribution is characterized by voids spanning all scales of the turbulent flow; their signature in the coarse-grained mass probability distribution is an algebraic behavior at small densities.

PACS numbers: 47.27.-i, 47.10.-g

Understanding the spatial distribution of finite-size massive impurities, such as droplets, dust or bubbles suspended in incompressible flows is a crucial issue in engineering [1], planetology [2] and cloud physics [3, 4]. Such particles possess inertia, and generally distribute in a strongly inhomogeneous manner. The common understanding of this long known but remarkable phenomenon of *preferential concentrations* relies on the idea that, in a turbulent flow, vortexes act as centrifuges ejecting particles heavier than the fluid and entrapping lighter ones [5, 6]. This picture was successfully used [5, 6, 7, 8, 9] to describe the small-scale particle distribution and to show that it depends only on the Stokes number $\mathcal{S}_\eta = \tau/\tau_\eta$ which is obtained by non-dimensionalizing the particle response time τ with the characteristic time τ_η of the small turbulent eddies.

In this Letter, we confirm that this mechanism is relevant to describe the particle distribution at length-scales which are smaller than the dissipative scale of turbulence, η . In particular, maximal clustering is found for Stokes numbers of the order of unity. However, we show that particle concentration experiences also very strong fluctuations in the inertial range of turbulence. In analogy with small-scale clustering, it is expected that for $r \gg \eta$ the relevant parameter is the local Stokes number $\mathcal{S}_r = \tau/\tau_r$, where τ_r is the characteristic time of eddies of size r [10]. Surprisingly, we present evidences that such dimensional argument does not apply to describe how particles organize in the inertial range of turbulence. We show that the way they distribute depends on the scale-dependent rate at which volumes are contracted.

In very dilute suspensions, small particles much heav-

ier than the fluid evolve according to the Newton equation [11]

$$\tau \ddot{\mathbf{X}} = \mathbf{u}(\mathbf{X}, t) - \dot{\mathbf{X}}, \quad (1)$$

where buoyancy is neglected. The response time τ is proportional to the square of the particles size and to their density contrast with the fluid. The fluid velocity \mathbf{u} satisfies the incompressible Navier-Stokes equation

$$\partial_t \mathbf{u} + \mathbf{u} \cdot \nabla \mathbf{u} = -\nabla p + \nu \nabla^2 \mathbf{u} + \mathbf{F} \quad \text{with} \quad \nabla \cdot \mathbf{u} = 0, \quad (2)$$

p being the pressure and ν the viscosity; \mathbf{F} is an external force that injects energy at large scales L with a rate $\varepsilon = \langle \mathbf{F} \cdot \mathbf{u} \rangle$. We performed direct numerical simulations of (2) by means of a pseudo-spectral code on a cubic grid of size $\mathcal{L} = 2\pi$ with 128^3 , 256^3 and 512^3 collocation points corresponding to Reynolds numbers (at the Taylor micro-scale) $R_\lambda \approx 65$, 105 and 180, respectively. Particles ($N = 7.5$ millions for each set of 15 different Stokes number in the range $\mathcal{S}_\eta \in [0.16:3.5]$), initially seeded homogeneously in space with velocities equal to the local fluid velocity, are evolved with (1) for about two large-scale eddy turnover times. After this time, a statistical steady state is reached and measurements are performed. Details on the numerics are reported in [12].

Below the Kolmogorov length-scale η where the velocity field is differentiable, the motion of inertial particles is governed by the fluid strain and their dissipative dynamics leads their trajectories to converge to a dynamically evolving attractor. For any given response time of the particles, their mass distribution is singular and generically scale-invariant with fractal properties at

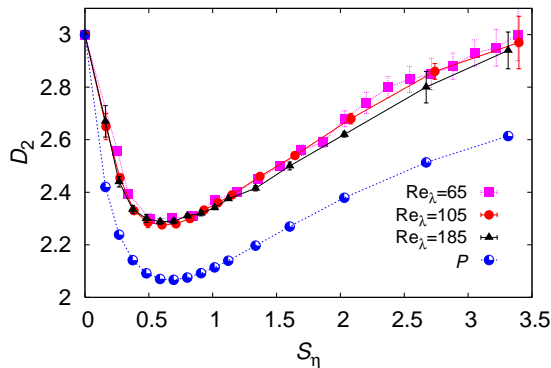


FIG. 1: (Color online) Correlation dimension \mathcal{D}_2 vs \mathcal{S}_η for the three different Re_λ , and probability \mathcal{P} to find particles in non-hyperbolic (rotating) regions of the flow, shown for $Re_\lambda = 185$ (multiplied by an arbitrary factor for plotting purposes). The correlation dimension \mathcal{D}_2 has been estimated taking into account also subleading terms, as described in [14].

small scales [13, 14]. In order to characterize such particle clusters we measured the correlation dimension \mathcal{D}_2 , which is estimated through the small-scale scaling behavior of the probability to find two particles at a distance less than a given r : $P_2(r) \sim r^{\mathcal{D}_2}$. The dependence of \mathcal{D}_2 on \mathcal{S}_η and Re_λ is shown in Fig. 1. We first notice that \mathcal{D}_2 depends very weakly on Re_λ at least in the range of Reynolds number here explored. This observation agrees with a recent numerical study [9], where particle clustering was equivalently characterized in terms of the radial distribution function. This indicates that τ_η , which varies by more than a factor 2 between the smallest and the largest Reynolds number considered here, is the relevant time scale to characterize clustering below η . For all values of Re_λ , a maximum of clustering (corresponding to a minimum of \mathcal{D}_2) is observed for $\mathcal{S}_\eta \approx 0.6$. For values of \mathcal{S}_η larger than those investigated here, \mathcal{D}_2 is expected to saturate to the space dimension [14]. For small values of \mathcal{S}_η particle positions strongly correlate with the local structure of the fluid velocity field. This is evidenced in Fig. 1 which displays the probability \mathcal{P} to find particles in non-hyperbolic regions of the flow, i.e. at those points where the strain matrix has two complex conjugate eigenvalues. Note that \mathcal{P} attains its minimum for values of \mathcal{S}_η close to the minimum of \mathcal{D}_2 . This supports the traditional view relating particle clustering to vortex ejection. As qualitatively evidenced from Fig. 2, particle positions correlate with low values of the fluid acceleration. This phenomenon was already evidenced in [12] where a statistical analysis of the fluid acceleration at particle positions is performed, and also in [15] for two-dimensional turbulent flows.

As seen from Fig. 2 the fluctuations in the particle spatial distribution extend far inside the inertial range. In particular, for Stokes numbers of the order of unity (Figs. 2c and d), one observes that the sizes of voids

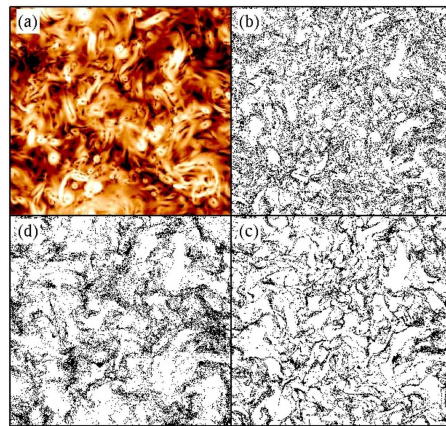


FIG. 2: (Color online) (a) Modulus of the pressure gradient, which gives the main contribution to fluid acceleration, on a slice $512 \times 512 \times 4$. B/W code low and high intensity, respectively. Particle positions in the same slice shown for (b) $\mathcal{S}_\eta = 0.16$, (c) 0.80 and (d) 3.30. Note the presence of voids with sizes much larger than the dissipative scale.

span all the active spatial scales of the fluid turbulent flow, as already observed in two-dimensional inverse cascade [15, 16]. To gain some quantitative insight on the particle distribution, we consider the pdf $P_{r,\tau}(\rho)$ of the particle density coarse-grained on a scale r inside the inertial range. For tracers, which are uniformly distributed, this pdf is a delta function centered on $\rho = 1$ for infinite number of particles $N \rightarrow \infty$. For a large but finite N , it is given by the asymptotic behavior of the binomial distribution, i.e. $P_{r,0}(n) \propto (\mathcal{L}^3/Nr^3) \exp[(Nr^3/\mathcal{L}^3)(\rho - 1 - \rho \ln \rho)]$. In our settings, the typical number of particles in cells inside the inertial range is several thousands. Finite number effects are thus not expected to affect the core of mass distributions $\rho = \mathcal{O}(1)$ but they may be particularly severe when $\rho \ll 1$ because of the presence of voids. To reduce this spurious effect, we actually computed the quasi-Lagrangian (QL) mass density pdf $P_{r,\tau}^{(QL)}(\rho)$, which corresponds to a Lagrangian average with respect to the natural measure, and is obtained by weighting each cell with the mass it contains. For statistically homogeneous distribution, QL statistics can be related to the more traditional Eulerian measurements by noticing that $\langle \rho_r^p \rangle_{QL} = \langle \rho_r^{p+1} \rangle$.

Figure 3 shows $P_{r,\tau}^{(QL)}(\rho)$ for various response times τ and at a given scale r within the inertial range. Deviations from a uniform distribution can clearly be observed; they become stronger and stronger as τ increases. The presence of such strong deviations shows that, at variance with the prediction of [13], concentration fluctuations are important not only at dissipative scales but also in the inertial range. A noticeable observation is that the low-density tail of the pdf (which is related to voids) displays an algebraic behavior $P_{r,\tau}^{(QL)}(\rho) \sim \rho^{\alpha(r,\tau)}$. This means that the Eulerian pdf of the coarse-grained mass density

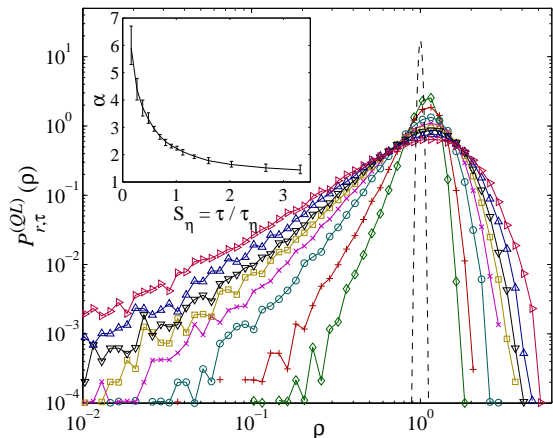


FIG. 3: (Color online) Quasi-Lagrangian pdf of the coarse-grained mass density ρ_r in log-log scale for $S_\eta = 0.27, 0.37, 0.58, 0.80, 1.0, 1.33, 2.03, 3.31$ (from bottom to top) at scale $r = \mathcal{L}/16 = 0.39$. The solid line represent the Poisson distribution. Inset: exponent of the power law left tail α vs S_η . The exponents have been estimated from a best fit of the cumulative probability which is far less noisy.

has also a power-law tail for $\rho \ll 1$ with exponent $\alpha - 1$. The dependence of such an exponent for fixed r and varying the Stokes number S_η is shown in the inset. For low inertia ($S_\eta \rightarrow 0$) the exponent tends to infinity in order to recover the non-algebraic behavior of tracers. At the largest Stokes numbers we have, the exponent seems to approach $\alpha = 1$, indicating a non-zero probability for totally empty areas. Note however that α is expected to go to infinity when $S_\eta \rightarrow \infty$ with r fixed since a uniform distribution must be recovered for infinite inertia. These algebraic tails are relevant to various physical/chemical processes involving heavy particles. For example, the growth of liquid droplets by condensation of vapor onto aerosol particles can be largely influenced by the distribution of low-density regions [13]. This is an important effect to be considered in the modelling of droplet growth and of aerosol scavenging [3, 4].

Fixing the response time τ and increasing the observation scale r reproduces the same qualitative picture as fixing r and decreasing τ . A uniform distribution is recovered in both limits $r \rightarrow \infty$ or $\tau \rightarrow 0$. These two limits are actually equivalent. At length-scales $r \gg \eta$ within the inertial range, the fluid velocity field is not smooth: according to the Kolmogorov 1941 (K41) theory, velocity increments behave as $\delta_r u \sim (\varepsilon r)^{1/3}$. Standard turbulence theory suggests that the physics at scale r is associated to time scales of the order of the turnover time $\tau_r = r/\delta_r u \sim \varepsilon^{-1/3} r^{2/3}$. It is then clear that, for any finite particle response time τ , the local inertia measured by $S_r = \tau/\tau_r$ becomes so small at sufficiently large scales that particles should behave as tracers and so distribute uniformly in space [10]. Deviations from uniformity for finite S_r are expected not to be scale-invariant [13]. In

particular, phenomenology suggests that the particle distribution should depend only on the local Stokes number S_r as observed in random δ -correlated in time flows [17]. However this argument does not take into consideration some important aspects of realistic flows.

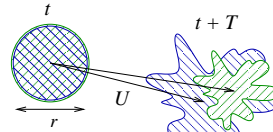


FIG. 4: Sketch of the time evolution of two blobs of tracers and inertial particles respectively. The tracers diffuse while the volume of particles contracts.

Consider two initially identical blobs of size r , one of tracers and one of inertial particles. They develop discrepancies originating from two effects (see Fig. 4). First, the two blobs are on average advected with different velocities: the tracers are swept by the large-scale velocity U , while the inertial particles have a delay due to their response time τ . This gives a relative displacement between the blobs of the order of $\tau U/r$, which expresses the ratio between the response time τ and the sweeping time r/U . Second, the blob of tracers, while advected, conserves the volume but is distorted with a typical time scale of order τ_r , whereas the particles possess also another time scale coming from the fact that the volume of the blob contracts with rate $1/\mathcal{T}_{r,\tau}$, not known a priori. Thus also the relative time $\tau_r/\mathcal{T}_{r,\tau}$ should enter the dynamics. The two non-dimensional ratios associated to these two effects are both going to zero in the limit of vanishing inertia (i.e. $\tau \rightarrow 0$ or $r \rightarrow \infty$). Being the particle dynamics a function of the two above time ratios, it is then natural to expect that to observe a universal behaviour – if any – for the mass dynamics when varying r and τ one needs to keep the balance between the two effects constant. This implies for the contraction rate to go as: $\mathcal{T}_{r,\tau} = C \tau_r r/(U \tau)$, C being a fixed constant.

According to the above discussion one expects that the only relevant time scale to describe the distribution of particles at a scale r is $\mathcal{T}_{r,\tau}$. Therefore, the pdf of the coarse-grained mass density should depend only on the contraction rate, which can be made non-dimensional multiplying it by the typical fluid velocity gradient, i.e.

$$\Gamma = \frac{\tau_\eta}{\mathcal{T}_{r,\tau}} \sim Re^{1/4} S_\eta \left(\frac{r}{\eta}\right)^{-5/3} \sim Re^{-1} S_\eta \left(\frac{r}{L}\right)^{-5/3} \quad (3)$$

Note that the limit of infinite Reynolds number is very sensitive on how the observation scale r is fixed. Keeping constant the ratio r/L one gets a vanishing contraction rate Γ and a uniform distribution. Conversely when r/η is kept constant, Γ tends to infinity which means that particle distribution is dominated by caustics [18].

Figure 5 shows $P_{r,\tau}^{(QL)}(\rho)$ for three choices of Γ obtained from different sets of values of r and τ . The different

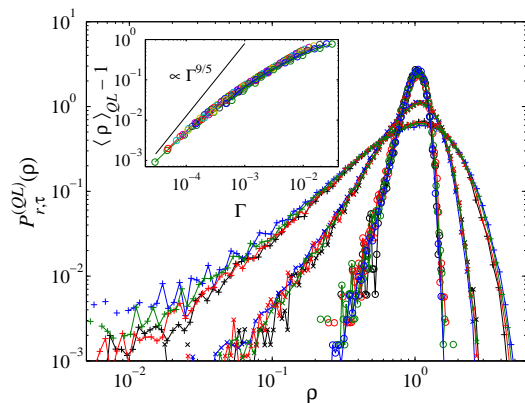


FIG. 5: (Color online) Pdf of the coarse-grained mass in the inertial range for three values of the non-dimensional contraction rate Γ . From bottom to top: $\Gamma = 4.8 \cdot 10^{-4}$ (different curves refer to $S_\eta = 0.16, 0.27, 0.37, 0.48$), $\Gamma = 2.1 \cdot 10^{-3}$ (for $S_\eta = 0.58, 0.69, 0.80, 0.91, 1.0$), $\Gamma = 7.9 \cdot 10^{-3}$ (for $S_\eta = 1.60, 2.03, 2.67, 3.31$). Inset: deviation from unity $\langle \rho \rangle_{QL} - 1$ of the first-order QL moment for scales r within the inertial range. For comparison, the behavior $\propto \Gamma^{9/5}$ obtained when assuming point clusters of particles is shown as a solid line.

curves collapse, demonstrating the above argument, i.e., that the only relevant time scale is given by the contraction rate $1/\mathcal{T}_{r,\tau}$. In particular, as represented in the inset of Fig. 5, the deviations from unity of the first moment of density collapse for all S_η investigated and for all scales inside the inertial range of our simulation. This quantity is the same as the Eulerian 2nd-order moment and gives the probability $P_2(r)$ to have two particles within a distance r . The particle distribution recovers uniformity at large scales very slowly: much slower than if they were distributed as Poisson point-like clusters, for which $\langle \rho^2 \rangle - 1 \propto r^{-3} \propto \Gamma^{9/5}$ (shown in the inset for comparison).

As we have seen, understanding how particle distribution recovers uniformity in the inertial range is equivalent to consider the asymptotics of small inertia. In this limit, particles almost behave as if they were advected by the compressible velocity field $\mathbf{v} = \mathbf{u} - \tau(\partial_t \mathbf{u} + \mathbf{u} \cdot \nabla \mathbf{u})$ [11]. The contraction rate $\mathcal{T}_{r,\tau}^{-1}$ is then given by the average of $\nabla \cdot \mathbf{v} \simeq \tau \nabla^2 p$ over a ball of radius r . This leads to $\mathcal{T}_{r,\tau}^{-1} \sim (\tau/r) \delta_r \nabla p$. When assuming that the scaling behavior of the pressure gradients increments is dominated by sweeping [19], namely $\delta_r \nabla p \sim U \varepsilon^{1/3} r^{-2/3}$, one straightforwardly obtains (3). This alternative way to obtain the scaling behavior of the volume contraction rate $\mathcal{T}_{r,\tau}^{-1}$ emphasizes the strong correlations between the structure of the acceleration field (and thus pressure) and the spatial distribution of particles in the inertial range. Other small scale quantities related to fluid velocity gradients, such as vorticity or eigenvalue of the strain matrix, play a lesser role than acceleration. Characterizing the distribution of acceleration is thus crucial

to understand particle clusters, and conversely, particle distribution could be used as experimental tool to probe the spatial structure of turbulent flows.

We acknowledge useful discussions with G. Boffetta, A. Celani and A. Fouxon. This work has been partially supported by the EU under contract HPRN-CT-2002-00300 and the Galileo programme on Lagrangian Turbulence. Simulations were performed at CINECA (Italy) and IDRIS (France) under the HPC-Europa programme (RII3-CT-2003-506079). The unprocessed data of this study are freely available from <http://cfd.cineca.it>.

-
- [1] C. Crowe, M. Sommerfeld, and Y. Tsuji, *Multiphase Flows with Particles and Droplets* (CRC Press, New York, 1998).
 - [2] I. de Pater and J. Lissauer, *Planetary Science* (Cambridge University Press, Cambridge, 2001).
 - [3] H. Pruppacher and J. Klett, *Microphysics of Clouds and Precipitation* (Kluwer Academic Publishers, Dordrecht, 1996).
 - [4] A. Kostinski and R. Shaw, *J. Fluid Mech.* **434**, 389 (2001).
 - [5] J. Eaton and J. Fessler, *Int. J. Multiphase Flow* **20**, 169 (1994).
 - [6] J. Fessler, J. Kulick, and J. Eaton, *Phys. Fluids* **6**, 3742 (1994).
 - [7] K. Squires and J. Eaton, *J. Fluid Mech.* **226**, 1 (1991).
 - [8] W. Reade and L. Collins, *Phys. Fluids* **12**, 2530 (2000).
 - [9] L. Collins and A. Keswani, *New J. Phys.* **6**, 119 (2004).
 - [10] G. Falkovich, A. Fouxon, and M. Stepanov, in *Sedimentation and Sediment Transport*, edited by A. Gyr and W. Kinzelbach (Kluwer Academic Publishers, Dordrecht, 2003), pp. 155–158.
 - [11] M. Maxey, *J. Fluid Mech.* **174**, 441 (1987).
 - [12] J. Bec, L. Biferale, G. Boffetta, A. Celani, M. Cencini, A. Lanotte, S. Musacchio, and F. Toschi, *J. Fluid Mech.* **550**, 349 (2006).
 - [13] E. Balkovsky, G. Falkovich, and A. Fouxon, *Phys. Rev. Lett.* **86**, 2790 (2001).
 - [14] J. Bec, M. Cencini, and R. Hillerbrand (2006), preprint.
 - [15] L. Chen, S. Goto, and J. Vassilicos, *J. Fluid Mech.* **553**, 143 (2006).
 - [16] G. Boffetta, F. De Lillo, and A. Gamba, *Phys. Fluids* **16**, L20 (2004).
 - [17] J. Bec, M. Cencini, and R. Hillerbrand (2006), preprint nlin.CD/0606038.
 - [18] M. Wilkinson and M. B., *Europhys. Lett.* **71**, 186 (2005).
 - [19] The scaling of pressure in the inertial range is actually a much debated issue. Tennekes [*J. Fluid Mech.* **67**, 561 (1975)] proposed that it does not follow K41 because of random sweeping, as also discussed by Nelkin and Tabor [*Phys. Fluids A* **2**, 81 (1990)] and supported by the experimental measurements of Van Atta and Wyngaard [*J. Fluid Mech.* **72**, 673 (1975)]. However, recent studies point out that two regimes are present (see, e.g., T. Gotoh and D. Fukayama, *Phys. Rev. Lett.* **86**, 3775, 2001).